

# Selectivity and activation of dopamine D3R from molecular dynamics

Zhiwei Feng · Tingjun Hou · Youyong Li

Received: 15 November 2011 / Accepted: 14 June 2012 / Published online: 3 July 2012  
© Springer-Verlag 2012

**Abstract** D<sub>3</sub> receptor, a member of dopamine (DA) D<sub>2</sub>-like receptor family, which belongs to class A of G-protein coupled receptors (GPCRs), has been reported to play a critical role in neuropsychiatric disorders. Recently, the crystal structure of human dopamine D<sub>3</sub> receptor was reported, which facilitates structure-based drug discovery of D<sub>3</sub>R significantly. We dock D<sub>3</sub>R-selective compounds into the crystal structure of D<sub>3</sub>R and homology structure of D<sub>2</sub>R. Then we perform 20 ns molecular dynamics (MD) of the receptor with selective compounds bound in explicit lipid and water. Our docking and MD results indicate the important residues related to the selectivity of D<sub>3</sub>R. Specifically, residue Thr<sup>7,39</sup> in D<sub>3</sub>R may contribute to the high selectivity of R-22 with D<sub>3</sub>R. Meanwhile, the 4-carbon linker and phenylpiperazine of R-22 improve the binding affinity and the selectivity with D<sub>3</sub>R. We also dock the agonists, including dopamine, into D<sub>3</sub>R and perform MD. Our molecular dynamics results of D<sub>3</sub>R with agonist bound show strong conformational changes from TM5, TM6, and TM7, outward movement of intracellular part of TM6, fluctuation of “ionic lock” motif and conformational change of Tyr<sup>7,53</sup>, which is consistent with recent crystal structures of active GPCRs and illustrates the dynamical process during activation. Our results reveal the mechanism of selectivity and activation for D<sub>3</sub>R, which is important for developing high selective antagonists and agonists for D<sub>3</sub>R.

**Keywords** Conformational changes · D<sub>3</sub> receptor · Mechanism of selectivity and activation · Molecular dynamics

## Introduction

The biogenic amine dopamine is a major neurotransmitter in the central nervous system that plays a critical role in movement, cognition, and emotion [1, 2]. Imbalance of the dopaminergic system is implicated in several neurological and neuropsychiatric disorders, such as Parkinson's disease, Huntington's disease, schizophrenia, Tourette's syndrome, and drug abuse [1, 3–7]. All dopamine receptor subtypes belong to class A of G-protein coupled receptors [8–10] (GPCRs) super family, and are divided into two families [11, 12] due to the basic pharmacological profiles: D<sub>1</sub>-like receptors including the dopamine D<sub>1</sub> and the D<sub>5</sub> receptors, are characterized by activation of adenylyl cyclase mediated by stimulatory G<sub>s</sub> protein, while D<sub>2</sub>-like receptors consist of the dopamine D<sub>2</sub>, D<sub>3</sub> and D<sub>4</sub> receptors, which couple to inhibitory G<sub>i/o</sub> proteins and inhibit adenylyl cyclase [13, 14].

The D<sub>3</sub> dopamine receptor is a member of the D<sub>2</sub>-like receptor family, which was discovered by Sokoloff and his colleagues in 1990 [15], reporting to play a critical role in neuropsychiatric disorders [16, 17]. It has been revealed to be a therapeutic target for antipsychotic and antiparkinsonian drugs. High degrees of sequence identities are within the trans-membrane helices among D<sub>2</sub>-like receptor [2, 13, 16, 18–21], especially between D<sub>2</sub>R and D<sub>3</sub>R. Importantly, the near-identity of the residues inferred to form the binding site among them produces a formidable challenge to developing D<sub>3</sub>R-selective compounds with drug-like physicochemical properties. It is a great challenge to identify selective dopamine D<sub>3</sub> receptor ligands with high binding affinities and understand the pharmacological role of D<sub>3</sub>R.

**Electronic supplementary material** The online version of this article (doi:10.1007/s00894-012-1509-x) contains supplementary material, which is available to authorized users.

Z. Feng · T. Hou · Y. Li (✉)  
Institute of Functional Nano & Soft Materials (FUNSOM)  
and Jiangsu Key Laboratory for Carbon-Based Functional  
Materials & Devices, Soochow University,  
Suzhou, Jiangsu 215123, China  
e-mail: yyli@suda.edu.cn

To date, some D3R-selective compounds have been developed and they are in ongoing clinical trials as potential therapeutics. BP 897 is initially identified as a partial agonist but later displays an antagonist property [22–26], SB 277011A [27–34], NGB 2904 [29, 32, 34–37], R-22 [1, 12, 38] and SB 269,652 [38–40] are classified into D3R-selective antagonist too.

Although, the structure-activity relationships (SARs) have been utilized to develop ligands for dopamine receptors, it is very difficult to design high selective compounds without high resolution crystal structure of dopamine receptors. Recently, the crystal structure of the human D3R was reported [1], which makes structure-based methodologies plausible to develop high selective compounds for D3R. We dock selective compounds and agonist into D3R and D2R and perform molecular dynamics. Our results reveal the mechanism of selectivity and activation for D3R, which is important for developing high selective antagonists and agonists for D3R. Section 2 is the methods. Section 3 includes the results and discussion. Section 4 is the summary.

## Methods

### Homology modeling

The crystal structure of human D3R (PDB entry: 3PBL, resolution 2.89 Å) [1] is used as the template to construct the human D1R, D2R and D4R receptors. The sequences of the human D1R, D2R and D4R are retrieved from GenBank (P21728, P14416, and P21917) (<http://www.uniprot.org/uniprot/>). The sequences are aligned based on the sequence analysis of dopamine D2-like receptor family. Then we build the homology model of D1R, D2R and D4R by using Discovery Studio [41]. Chain A of D3R in the crystal structure is used as the template to build the homology models.

Once the 3D models are generated, energy minimization is performed for these receptors before dockings and molecular dynamics simulations. Structural evaluation and stereochemical analyses are performed using proSA-web Z-scores [42] and PROCHECK Ramachandran plots [43]. Furthermore, root mean squared deviation (RMSD), superimposition of query and template structure, and visualization of generated models are performed using UCSF Chimera 1.5.3 [44].

Histidine residue is the only one which ionizes within the physiological pH range (~7.4). To determine the protonation states for histidines, we use “the PROPKA web interface” to predict protein ionization and residue pKa values. Compared with the pKa of histidines in the output file, we find all the pKa values of histidines (5.86, 6.38, 5.11, 6.48, and 6.42, respectively) are lower than the pKa value of the model (6.50), especially the pKa value of His<sup>6.55</sup> is the lowest (5.11), so we decide not to protonate the histidines.

### Construction for the 3D model of receptor-ligand complex

The dock program CDocker and DS [41] Catalyst Score are applied to construct receptor-ligand complexes. The center of the binding site of the receptor is set at the center of the ligand in the crystal structure of human D3R with a radius of 13 Å, large enough to cover the binding pocket. CDocker [41] is a grid-based molecular docking method that employs CHARMM [45]. The receptor is held rigid while the ligands are allowed to flex during the refinement. For pre-docked ligands, prior knowledge of the binding site is not required. It is possible, however, to specify the ligand placement in the active site using a binding site sphere. Random ligand conformations are generated from the initial ligand structure through high temperature molecular dynamics, followed by random rotations. The random conformations are refined by grid-based simulated annealing and a final grid-based or full forcefield minimization. The RMSD between our docking structure of D3R with doxepin by using CDocker [41] and the crystal structure is 1.23 Å, more details can be found in supplementary Fig. S1.

### MD simulations

The proteins are embedded in a pre-equilibrated (66 by 66 Å) and periodic structure of 1-palmitoyl-2-oleoyl-sn-glycero-3-phosphatidylcholine (POPC). The lipid molecules within 5 Å of the complex are eliminated. Then we insert it into a water box (TIP3P [46] water model) and eliminate the waters within 5 Å of the lipid and protein. The molecular dynamics simulation system is built up by using VMD [47–51].

The whole system (Fig. 1) includes the protein, 100 lipid molecules, ~6617 water molecules, and eight chlorine ions for a total of ~31,961 atoms per periodic cell. The box size is 66 Å by 66 Å by 75 Å. The system is first equilibrated for 500 ps with the protein fixed. Then the protein is released and another 500 ps equilibration is performed.

Starting from the last frame of the equilibration, we perform 20 ns molecular dynamics simulation. Three independent MD trajectories of each system are performed in the present work. The MD simulations are performed using the NAMD [52] package (version 2.7b2) with CHARMM27 [45, 53, 54] force field for the studied complex with explicit water and periodically infinite lipid. Electrostatics are calculated using the particle mesh Ewald [55] (PME) method with a 12 Å non-bonded cutoff and a grid spacing of 1 Å per grid point in each dimension. The van der Waals energies are calculated using a smooth cutoff (switching radius 10 Å, cutoff radius 12 Å). The temperature and pressure are kept constant using a langevin thermostat and langevin barostat, respectively. The time step of three independent MD trajectories of each system is set to 1 fs. The data is saved every 10 ps for analysis. 20 ns MD simulation is performed under a constant temperature of 310 K and a

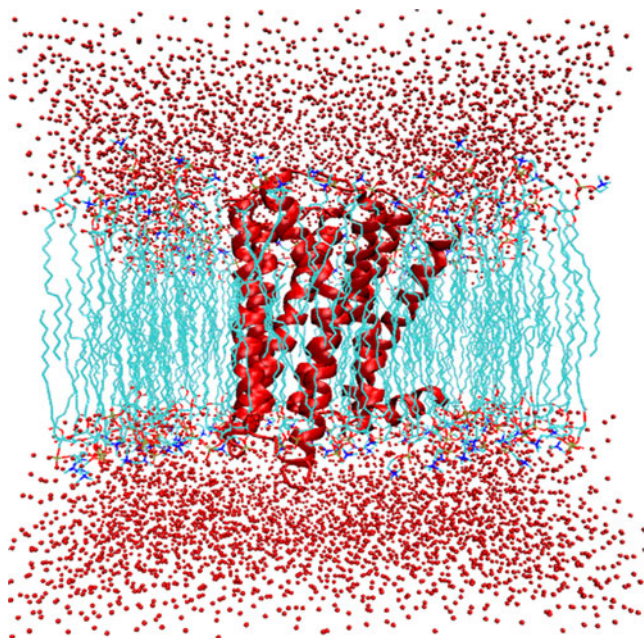


**Fig. 1** The molecular dynamics simulation box of D3R with lipid and water. The snapshot shown above is after 20 ns of equilibration. The EC region is at the top

constant pressure of 1 atm. Trajectory analyses are carried out with VMD [47].

## Results and discussion

### Area per lipid and membrane thickness

In the molecular modeling study of a lipid bilayer, the cross-sectional area per lipid and the membrane thickness are adequate indicators of the bilayer thermal equilibration.

Bilayer thickness is evaluated as the distance between the average positions of phosphorus atoms in the two leaflets of a bilayer. The average phosphorus-phosphorus distance in the POPC bilayer is  $40.5 \pm 1.6$  Å (three independent trajectories of each system). Average cross-sectional area/POPC is  $\sim 63.9 \pm 1.3$  Å<sup>2</sup> in POPC bilayer. The values of cross-sectional area per lipid and the membrane thickness is in agreement with the recent study [56], and three independent simulations of each system share most of the similarities (see the following discussions), which indicates our system is equilibrated. Snapshot of the POPC bilayer at the end of the respective 20 ns trajectory is shown in Fig. 2.

### Sequence similarity and structure similarity among D<sub>2</sub>-like receptor family

As members of the class A rhodopsin-like GPCRs, D<sub>2</sub>-like receptors share the same topology and important motifs, which are composed of seven trans-membrane helices

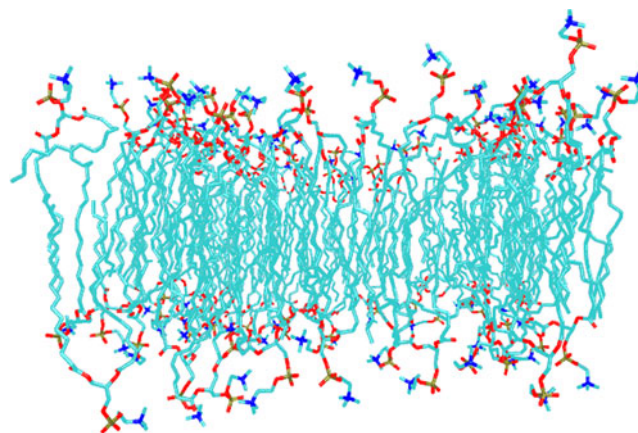


**Fig. 2** Snapshot of the POPC bilayer at 20 ns of MD simulation

(TM1-TM7) connected by intracellular loops (IL1-IL3) and extracellular loops (EL1-EL3). According to the known crystal structures including crystal structure of the human D3R, another short helix (TM8), is directly connected to the seventh trans-membrane helix. The huge intracellular loop 3 (IL3) is the main difference among the D<sub>2</sub>-like receptors. Several splice variants have been revealed on the different subtypes based on the IL3: there are three splice variants of the D<sub>2</sub> receptors (D<sub>2short</sub>, D<sub>2long</sub> and D<sub>2longer</sub>), two variants of D<sub>3</sub> receptors for mice (D<sub>2L</sub> and D<sub>2S</sub>), and several truncated isoforms and a frame-shifted splice variant (D<sub>3nf</sub>) in human, while D<sub>4</sub> receptors have three polymorphic variations including D<sub>4.2</sub>, D<sub>4.4</sub> and D<sub>4.7</sub>.

A sequence alignment of the D<sub>1</sub> and D<sub>2</sub>-like receptors reveals a moderate sequence identity:  $\sim 28$  % between D<sub>2</sub> and D<sub>4</sub>,  $\sim 29.3$  % between D<sub>3</sub> and D<sub>4</sub> receptors, while the sequence identity between D<sub>3</sub> and D<sub>2</sub> receptors is significantly high ( $\sim 44$  %). Sequence similarities are higher than sequence identities: 40.2 % for D<sub>2</sub>/D<sub>4</sub>, 41 % for D<sub>3</sub>/D<sub>4</sub> and 51 % for D<sub>3</sub>/D<sub>2</sub>. Focusing on the TM regions as the relevant interaction sites for ligand recognition, sequence identity is increased to 50.2 % for D<sub>2</sub>/D<sub>4</sub>, 53 % for D<sub>3</sub>/D<sub>4</sub> and 79 % for D<sub>3</sub>/D<sub>2</sub> receptors. Sequence similarities are 72 % for D<sub>2</sub>/D<sub>4</sub>, 73 % for D<sub>3</sub>/D<sub>4</sub> and 90 % for D<sub>3</sub>/D<sub>2</sub> receptors, respectively. Due to the high sequence similarity between D<sub>2</sub> and D<sub>3</sub> receptors, it remains a challenging task to develop D<sub>3</sub>/D<sub>2</sub> selective compounds. The recent crystal structure of D3R provides us the structure information to develop D<sub>3</sub>/D<sub>2</sub> selective compounds and facilitates drug development for D<sub>2</sub>-like receptors significantly.

### Binding of antagonists and selectivity of D3R

Using the recent crystal structure of the human D3R as template, we construct homology models of D<sub>1</sub>, D<sub>2</sub> and D<sub>4</sub> receptors. Chain A of D3R in the crystal structure is used as the template to build the homology models.



After minimization of the four receptors and D3R-selective compounds, which include BP 897, NGB 2904, R-22, SB 277011A and SB 269,652, we use CDOCKER program in Discovery Studios to dock the ligands into the four receptors (Table 1).

Our docking results (Table 1) show that the docking scores of CDOCKER\_Energy of BP 897 with D<sub>3</sub>, D<sub>1</sub>, D<sub>4</sub> and D<sub>2</sub> receptors are -22.5, -6.8, 8.7 and 12.2 kcal mol<sup>-1</sup>, respectively. The CDOCKER\_Energies indicate that BP 897 binds stronger to D<sub>3</sub> receptor than other receptors, which is consistent with binding affinities. BP 897 binds into dopamine D<sub>3</sub> receptor with high affinity (K<sub>i</sub>=1.1 nM). Meanwhile, BP 897 binds dopamine D<sub>2</sub> receptor with lower affinity (K<sub>i</sub>=61 nM), which shows that BP 897 is a high selective compound for D<sub>3</sub> receptor.

CDOCKER\_Energies of NGB 2904 with D<sub>3</sub>, D<sub>1</sub>, D<sub>4</sub> and D<sub>2</sub> receptors are -11.1, 16.3, 39.7 and 31.8 kcal mol<sup>-1</sup>, respectively. NGB 2904 binds selectively to D<sub>3</sub> receptor, and binds stronger to D<sub>2</sub> than D<sub>4</sub>. This agrees with the SAR results: the binding affinity of NGB 2904 with D<sub>3</sub> receptor is (K<sub>i</sub>=1.4 nM) and NGB 2904 binds D<sub>3</sub> receptor 150-fold stronger than D<sub>2</sub> receptor, >800-fold stronger with rat D<sub>3</sub> than with rat D<sub>2</sub> receptor.

CDOCKER\_Energies of R-22 with D<sub>3</sub>, D<sub>1</sub>, D<sub>4</sub> and D<sub>2</sub> receptors are -31.9, -21.4, 16.6 and -3.1 kcal mol<sup>-1</sup>, respectively. R-22 shows it binds D<sub>3</sub> with the highest affinity (K<sub>i</sub>=1.1 nM) and binds 394-fold stronger with D<sub>3</sub> than D<sub>2</sub> receptor or D<sub>4</sub> receptor (D<sub>2</sub>:K<sub>i</sub>=433 nM/ D<sub>4</sub>:K<sub>i</sub>=3433 nM).

For SB 277011A, CDOCKER\_Energies with D<sub>3</sub>, D<sub>1</sub>, D<sub>4</sub> and D<sub>2</sub> receptors are -19.9, 18.9, 34.9 and 91.7, respectively. SB 277011A is a potent (K<sub>i</sub>=10 nM) and selective (~100-fold vs D<sub>2</sub>) D<sub>3</sub> receptor antagonist and has been reported to be at least 100-fold selective over 60 receptors including other D<sub>2</sub>-like receptors.

CDOCKER\_Energies of SB 269,625 with D<sub>3</sub>, D<sub>1</sub>, D<sub>4</sub> and D<sub>2</sub> receptors are -32.9, -3.55, 19.5 and 25.6 kcal mol<sup>-1</sup>, respectively. The pK<sub>i</sub> of SB 269,625 with hD<sub>2</sub>, hD<sub>3</sub> and hD<sub>4</sub> are 5.04, 8.73, and <5 respectively.

These results indicate that these five ligands are selective for D<sub>3</sub> receptor. In order to understand the mechanism of the

selectivity, we dock R-22 to the crystal structure of D<sub>3</sub> receptor and homology structure of D<sub>2</sub> receptor in the same binding site, as shown in Fig. 3.

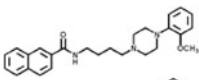
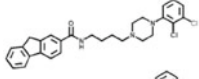
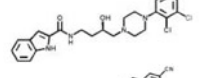
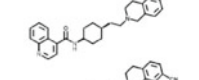
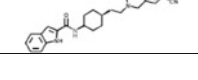

To compare the residues involved in binding R-22 from D<sub>2</sub>R and D<sub>3</sub>R, we align the binding sites as shown in Fig. 4. We can see that the core part of R-22 (2,3-diCl-phenylpiperazine) locates among the TM3, TM5, and TM6, whereas the indole-2-carboxamide terminus is oriented toward the extracellular part of the binding pocket composed by EL2 and the junction of TM1, TM2 and TM7.

Our results show that Asp<sup>3.32</sup> of D<sub>3</sub>R or D<sub>2</sub>R interacts strongly with R-22 (forming the salt bridge), and Asp<sup>3.32</sup> is conserved in many GPCRs.

Our results also show that Val<sup>3.33</sup>, Trp<sup>6.48</sup>, Phe<sup>6.51</sup>, Phe<sup>6.52</sup> and His<sup>6.55</sup> form favorable interactions with R-22. This agrees with the recent docking experiments [16–18, 20, 23, 25, 26, 29, 30, 57, 58], which show that the D<sub>3</sub> ligands bind to a primary recognition site provided by crucial microdomains of TM3, TM5 and TM6 and form favorable contacts with Asp<sup>3.32</sup>, Val<sup>3.33</sup>, Trp<sup>6.48</sup>, Phe<sup>6.51</sup>, Phe<sup>6.52</sup> and His<sup>6.55</sup>. Our docking results are consistent with mutation results. V3.33S significantly decreases the binding affinity of the ligands [4, 16, 18]. Mutation of F6.51A (~33.7-fold) or F6.51C (~83.5-fold) also affects the binding significantly [4, 16, 18]. W6.48 C leads to more than a 1350-fold decrease of the affinity [4, 16, 18]. Meanwhile, H6.55A causes a 180-fold increase of the binding affinity, and H6.55L in the D<sub>3</sub>R will decrease the binding affinity significantly [4, 16, 18]. Based on our docking results, a substantial destabilization of the aromatic cluster in TM6 is responsible for the effects of these mutations.

We find that two important residues in EL2 interact directly with R-22 in D<sub>3</sub>R, Cys<sup>5.31</sup> (Cys<sup>181</sup>) and Ser<sup>5.32</sup> (Ser<sup>182</sup>), which correspond to Cys<sup>5.31</sup>, and Ile<sup>5.32</sup> in D<sub>2</sub>R. Ser<sup>5.32</sup> in D<sub>3</sub>R interacts directly with R-22, but not for the corresponding residue Ile<sup>5.32</sup> in D<sub>2</sub>R. Meanwhile, recent SARs studies show

**Table 1** The docking scores of different ligands to different receptors

		D1R	D2R	D3R	D4R
BP 897		-6.8	12.2	-22.5	8.7
		kcal/mol	kcal/mol	kcal/mol	kcal/mol
NGB 2904		16.3	31.8	-11.1	39.7
		kcal/mol	kcal/mol	kcal/mol	kcal/mol
R-22		-21.4	-3.1	-31.9	16.6
		kcal/mol	kcal/mol	kcal/mol	kcal/mol
SB		18.9	91.7	-19.9	34.9
277011A		kcal/mol	kcal/mol	kcal/mol	kcal/mol
SB 269,625		-3.55	25.6	-32.9	19.5
		kcal/mol	kcal/mol	kcal/mol	kcal/mol

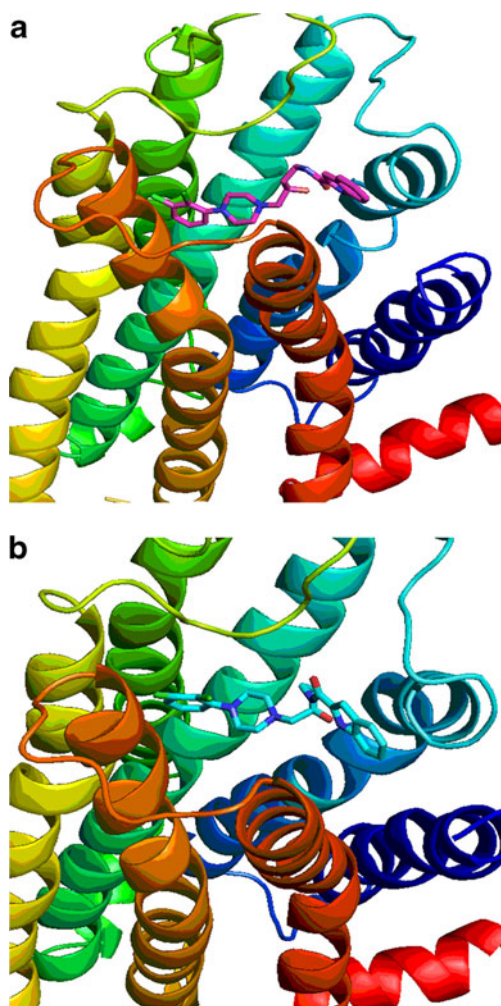


**Fig. 3** **a** The binding mode of R-22 with D3R. **b** The binding mode of R-22 with D2R

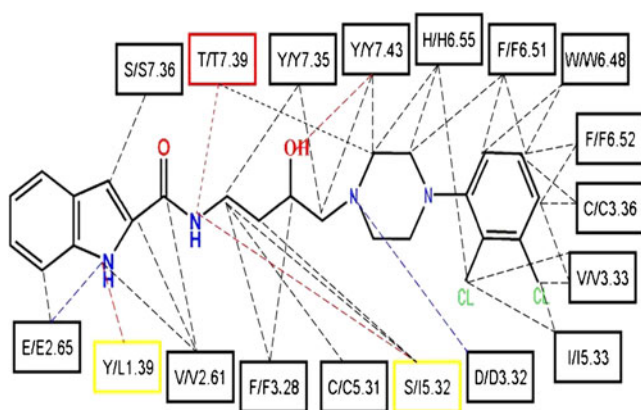


**Fig. 4** The residues involved in binding R-22 from D3R and D2R. For each residue pair, the former is from D3R, and the latter is from D2R. The selective residues for R-22 with D3R are highlighted in red or yellow. Hydrophobic contacts are shown in gray dashed lines, hydrogen bonds are highlighted in red dash lines, and salt bridges are highlighted in blue dash lines

that Ser<sup>5.32</sup> at the D3R is involved in D<sub>2</sub>/D<sub>3</sub> subtype selectivity, which is supported by our docking results.

In addition, we find that Tyr<sup>7.35</sup>, Ser<sup>7.36</sup>, Thr<sup>7.39</sup>, Tyr<sup>7.43</sup>, Tyr<sup>1.39</sup>, Val<sup>2.61</sup> and Glu<sup>2.65</sup> also contact with R-22, which is in agreement with the recent molecular docking experiments [4, 14, 16, 18, 20]. Those docking results showed that Tyr<sup>7.35</sup>, Ser<sup>7.36</sup> and Thr<sup>7.39</sup> in D3R represent a prominent part of the binding pocket in TM7 [4, 14, 18, 20]. It is reported that Y7.35V mutation causes 3.9-fold decrease of ligand binding. Mutation of T7.39V in D3R increases the binding affinity of 7-OH-DPAT [4, 14, 18, 20]. We find that Thr<sup>7.39</sup> in D2R does not interact with the ligand while the Thr<sup>7.39</sup> in D3R directly interacts with R-22. We find Tyr<sup>1.39</sup> in D3R interacts with R-22, which corresponds to the residue leucine in D2R. Our results highlight the critical difference between the binding pocket in D3R and D2R.

For the other four ligands: BP 897, NGB 2904, SB 277011A and SB 269,652, we find that Phe<sup>3.28</sup> and Val<sup>3.29</sup> from TM3, Val<sup>2.61</sup> and Leu<sup>2.64</sup> from TM2, and several residues from EL2: Val<sup>5.30</sup>, Cys<sup>5.31</sup> and Ser<sup>5.32</sup> (Val<sup>180</sup>, Cys<sup>181</sup>, and Ser<sup>182</sup>) form critical contacts with ligands. Recent mutagenesis and preliminary docking studies [4, 14, 16, 18, 20, 58] suggest that these residues are in proximity to the spacer elements and the heterocyclic appendages of the ligands, which contributes to subtype selectivity significantly. Our docking results also show that SB 277011A and SB 269,652 interact with three conserved residues, Ser<sup>5.46</sup>, Ser<sup>5.43</sup> and Ser<sup>5.42</sup>, which agrees with SARs studies [4, 18]. Soriano-Ursua and coworkers [59] reported a dopamine D2R model obtained from homology starting with the crystallized D3R recently. Our docking results are supported by their studies, which had a similar binding mode and most of the residues involved in the binding pocket [59]. SARs studies [4, 18] show that Ser<sup>5.46</sup>, Ser<sup>5.43</sup> and Ser<sup>5.42</sup> are of crucial importance for the binding affinity. These mutation results agree with our docking results.

In conclusion, our docking results of R-22, BP 897, NGB 2904, SB 277011A and SB 269,652 with D3R and D2R are supported by mutation results, SAR studies and consistent with preliminary docking results. Our results highlight the critical difference between the binding pocket in D3R and D2R, which includes T/T<sup>7.39</sup>, S/I<sup>5.32</sup> and Y/L<sup>1.39</sup>. Thr<sup>7.39</sup> and Tyr<sup>1.39</sup> form hydrogen bonds with R-22, respectively, while the corresponding residues Thr<sup>7.39</sup> and Leu<sup>1.39</sup> do not.

Molecular dynamics study of the complex of D3R with eticlopride

The complex of D3R with eticlopride is the first crystal structure of dopamine receptor family, which is in an inactive state. We first perform molecular dynamics on this complex to study the underlying mechanism.

During 20 ns molecular dynamics, the RMSD of three independent trajectories of the system is equilibrated within 4 ns as shown in Fig. S2. 20 ns is a reasonable time scale for our purpose to compare the differences for D3R with different ligands bound (we chose the RMSD of D3R with Eticlopride/R-22/Dopamine for clarify, and we find all the independent simulations are equilibrated within 4 ns).

Our molecular dynamics results show that three important residues: Ser<sup>5.32</sup>, Asp<sup>3.32</sup> and His<sup>6.55</sup> directly interact with the ligand. Figure 5 shows the time evolution for the hydrogen bond distances of them in two of three

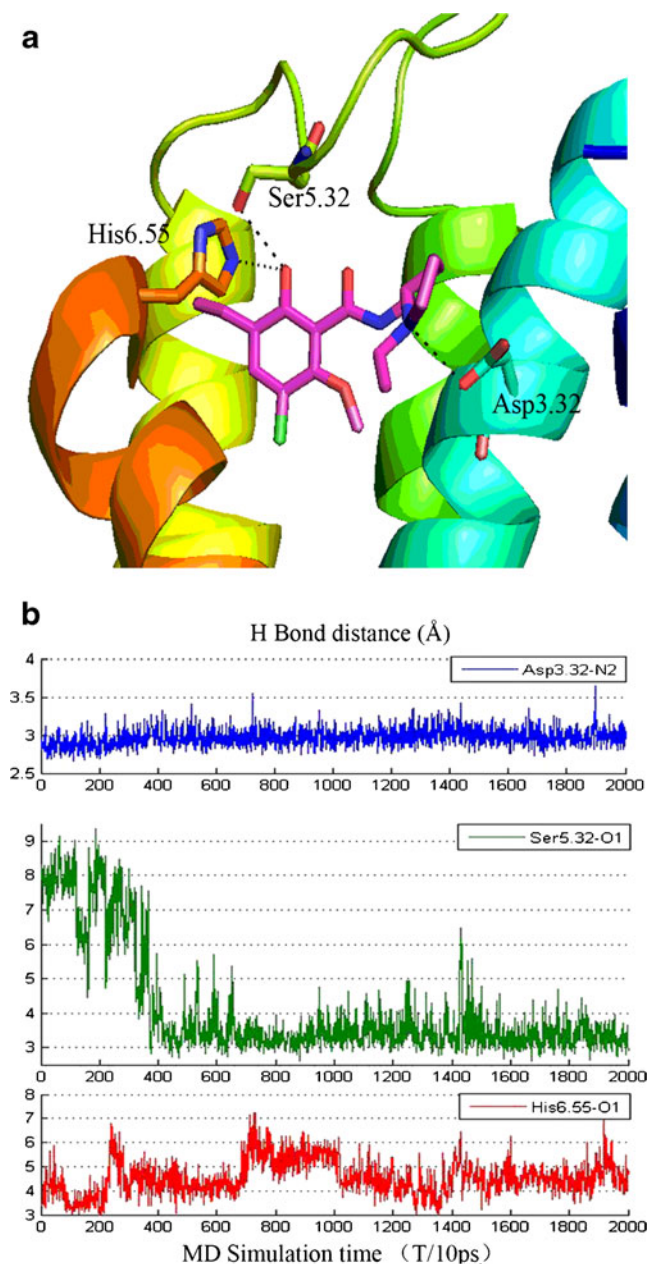


**Fig. 5** **a** The binding pose of eticlopride with D3R after 20 ns MD. **b** Evolution of the O-N/O-O distances between eticlopride and Asp3.32, Ser5.32 and His6.55 for 20 ns MD simulation

independent trajectories, and these two independent trajectories have the same results as shown in Fig. 5. While a subtly different situation of the third trajectory is shown in Fig. S3.

In Fig. 5, Asp<sup>3.32</sup> in the D3R forms a stable salt bridge with eticlopride during 20 ns MD. In addition, Asp<sup>3.32</sup> forms a stable H-bond with Tyr<sup>7.43</sup>. Ser<sup>5.32</sup> is 7~9 Å from the ligand initially and moves to ligand within 5~8 Å after 2 ns, then remains stable within 3.5 Å after 4 ns. Compared with the binding poses before molecular dynamics and after it, we can see that before molecular dynamics, the residue His<sup>6.55</sup> directly interacts with the ligand, while the residue Ser<sup>5.32</sup> is far from it. However, the hydrogen bond distance between His<sup>6.55</sup> and -O1 becomes larger and that between Ser<sup>5.32</sup> and -O1 becomes smaller during MD. Thus, Ser<sup>5.32</sup> interacts tightly with the ligand instead of His<sup>6.55</sup>.

However, in Fig. S3, our results show a subtly different situation of the third trajectory. Asp<sup>3.32</sup> in D3R also forms a stable salt bridge with eticlopride during 20 ns MD. Ser<sup>5.32</sup> gradually moves toward and forms a tight hydrogen bond with the ligand. Differently, His<sup>6.55</sup> keeps a stable interaction with ligand during our simulation.

Figure S4 shows time evolution of the important interhelical hydrogen bonds formed between TM127, TM234, and TM36. The hydrogen bond distances of conserved residues, such as Ser3.39-Asp2.50, Asp2.50-Ser7.46, Ser7.46-Asn1.50, Asn3.42-Ser2.45, Trp4.50-Ser2.45, and the ionic lock motif Arg3.50-Glu6.30 (Fig. S4c), remain stable with distance about 3 Å.

#### Molecular dynamics study of the complex of D3R with R-22

Similar as the complex of D3R with eticlopride, we performed 20 ns MD simulation of the complex D3R-R-22. The RMSD of the system is equilibrated within 4 ns as shown in Fig. S2 too. Importantly, our results show that R-22 has the same conformation in our three dependent MD simulations. Figure 6 and Fig. S5 show that the important residues form stable interaction during 20 ns MD, indicating R-22 has the same conformation in three independent simulations.

Figure 6a illustrates that the hydrogen bond distance of Asp<sup>3.32</sup> and -NH23 of ligand remains stable. The hydrogen bond distance between Tyr<sup>7.43</sup> and -OH30 of ligand starts at 3.5 Å initially and is stable at 3~4.5 Å. While the hydrogen bond distance of Thr<sup>7.39</sup> and -N18 fluctuates between 4 Å and 5 Å most of the time. We find that during the first 12 ns MD, Tyr<sup>1.39</sup> tightly interacts with Glu<sup>2.65</sup>, making the hydrogen bond between Glu<sup>2.65</sup> and -NH13 stable. After 12 ns MD, Glu<sup>2.65</sup> is no longer interacting with -NH13, while the residue Tyr<sup>1.39</sup> interacts directly with -NH13, which



**Fig. 6** **a** Evolution of the O-N/O-O distances between R22 and Asp3.32, Tyr7.43, Glu2.65, Tyr7.43, and Tyr1.39 for 20 ns MD simulation. These H-bonds are stable. **b** The binding pose of R-22 with D3R after 20 ns MD. **c** Schematic view of the interactions between R-22 and D3R after 20 ns MD: hydrophobic contacts are shown in gray dashed lines, hydrogen bonds are highlighted in red, and salt bridges are highlighted in blue. The residue highlighted in red interacts with R-22 in D3R, which contributes to the high selectivity of R-22 with D3R

confirms the important interactions formed between R-22 and these residues in D3R.

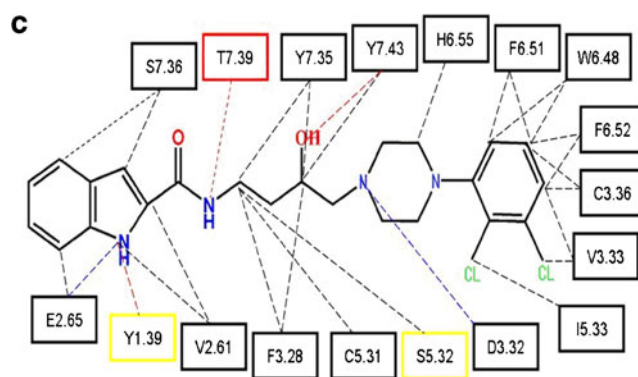
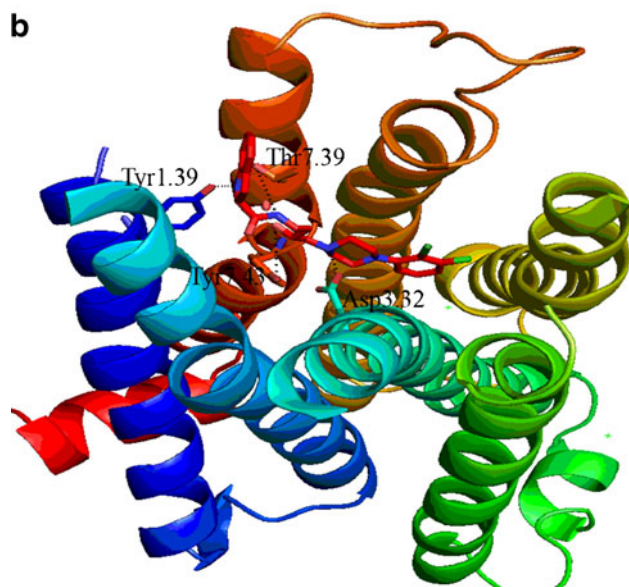
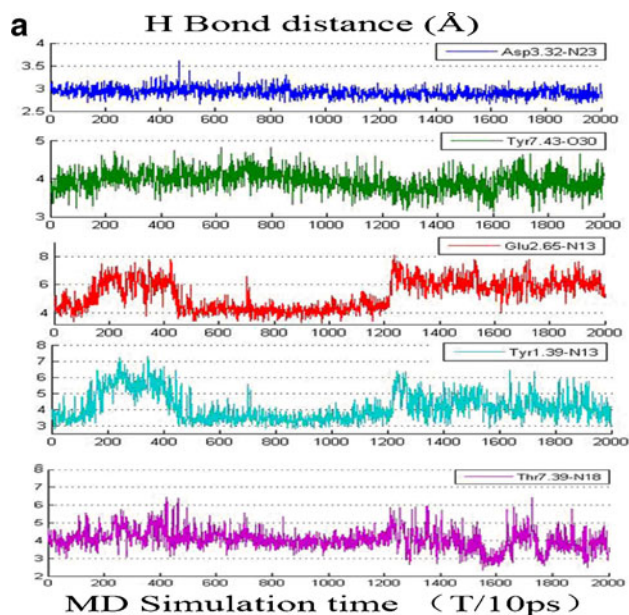
R-22 and eticlopride are two different ligands, but we can find similarities in their binding pockets. First, the ethylpyrrolidine part of eticlopride and the piperazine part of R-22 directly interacts with Asp<sup>3.32</sup> in D3R. Moreover, the aromatic ring of both fits tightly within a hydrophobic cavity formed by Val<sup>3.33</sup>, Phe<sup>6.51</sup>, Phe<sup>6.52</sup>, Ser<sup>5.42</sup> and Ser<sup>5.43</sup>. Figure S6 shows more similarities. There are differences between them too. First, the binding pocket of eticlopride is formed by helicesII, III, V, VI and VII, while that of R-22 includes an extracellular part consisting of helicesI, II and VII. Moreover, different residues play important but different roles: Ser<sup>5.32</sup> interacts with eticlopride while Thr<sup>7.39</sup> (or Tyr<sup>1.39</sup>) is more important for R-22.

Molecular dynamics study of the complex of D3R with its selective compounds

In order to compare the similarities and differences between D3R's selective compounds, we perform 20 ns MD of the complexes of D3R with BP 897, NGB 2904, SB 277011A and SB 269,652, respectively.

Our results show each ligand has the similar conformation in three independent MD simulations. Figure S7 shows many similarities among the five structures. First, in our docking experiments, all ligands share the similar binding mode. Second, hydrogen bond distance between residue Asp<sup>3.32</sup> and -NH of the ligand in all structures remains stable during 20 ns MD. The hydrogen bond distance of “ionic lock” motif Arg3.50-Glu6.30 is stable accompanying with little fluctuation. Importantly, highly conserved residues including Asn<sup>1.50</sup>, Asp<sup>2.50</sup>, Ser<sup>3.39</sup>, Trp<sup>6.48</sup>, Asn<sup>7.45</sup> and Ser<sup>7.46</sup> form inter-helical hydrogen bonds among TM12367 regions and these hydrogen bond distances keep stable during our MD.

When focusing on the complex of D3R with R22 and with SB 269,652, our molecular dynamics results show that the residue Glu<sup>2.65</sup> and Tyr<sup>1.39</sup> in D3R directly interacts with -NH of the ligands initially. With the backbone of R-22 undergoing conformational changes, both location and the dihedral angle of residue Glu<sup>2.65</sup> and Tyr<sup>1.39</sup> are different during molecular dynamics. As shown in Fig. S8, in the complex of D3R with SB 269,652, residue Glu<sup>2.65</sup> tightly interacts with -NH of ligand, while the residue Tyr<sup>1.39</sup> does



not. The situations of these two residues are different in the complex of D3R with R-22. A hydrogen bond forms between Glu<sup>2.65</sup> and -NH of R-22 during the first 12 ns,

while Tyr<sup>1.39</sup> interacts with the -NH after 12 ns. A main reason is the interaction between Tyr<sup>7.43</sup> and -OH of R-22 (more details in Fig. S8). Meanwhile, our results show that the other three ligands keep stable during 20 ns MD.

Figure S9 and Fig. S4b show that inter-helical hydrogen bonds form and keep stable in TM234 regions. The hydrogen bond distances among TM234 regions only exist in the complex of D3R with R-22.

#### Binding of agonists with D3R

In order to study the differences of binding pocket between antagonist and agonist, we dock two agonists (dopamine and apomorphine) to D3R and compare the results with antagonist docking results. As shown in Fig. 7a, dopamine and apomorphine share similar binding modes with D3R. The protonated nitrogen atom of the agonist forms a salt bridge with the conserved negatively charged Asp<sup>3.32</sup>. Both agonists bind tightly to Ser<sup>5.42</sup> and Ser<sup>5.46</sup>. Recently, Andujar and coworkers [60] reported the probable biologically relevant conformation of dopamine interacting with the D2R, and our binding mode is similar to their studies, where dopamine interacts with Asp<sup>3.32</sup> and Ser<sup>5.42</sup>. However, in the present work, we find that Ser<sup>5.46</sup> (or His<sup>6.55</sup>) forms a hydrogen bond with dopamine, while they found Ser<sup>122</sup> in TM4 formed a hydrogen bond with dopamine, which may be the main difference between D3R and D2R. Moreover, both dopamine and apomorphine form hydrophobic interactions with residues Val<sup>3.29</sup>, Val<sup>3.33</sup>, Cys<sup>3.36</sup>, Ile<sup>5.33</sup> (Ile<sup>183</sup>), Ser<sup>5.43</sup>, Trp<sup>6.48</sup>, Phe<sup>6.51</sup>, Phe<sup>6.52</sup> and His<sup>6.55</sup>, which agree with recent docking results [57, 61].

Our docking results show that Asp<sup>3.32</sup>, Ser<sup>5.42</sup>, Ser<sup>5.46</sup>, His<sup>6.55</sup> and some hydrophobic residues: Phe<sup>6.51</sup>, Phe<sup>6.52</sup> and Val<sup>3.33</sup> in D3R are significantly involved in binding agonist or antagonist.

#### Molecular dynamics study of the complex of D3R with its agonist dopamine

In order to differentiate the binding between agonist bound D3R and antagonist bound D3R and study the activation mechanism of D3R, we perform molecular dynamics simulation for D3R-agonist complex. First, we find that the RMSDs of three independent trajectories of the system are equilibrated within 4 ns as shown in Fig. S2.

Our results show that in three independent simulations, dopamine is stable and keeps tight interactions with D3R. Figure 7a and Fig. S10 show that in all simulations of D3R with dopamine, dopamine has the same conformation: the important residue Asp<sup>3.32</sup> in the D3R interacts with dopamine, and the hydrogen bond distance between Asp<sup>3.32</sup> and ligand remains stable

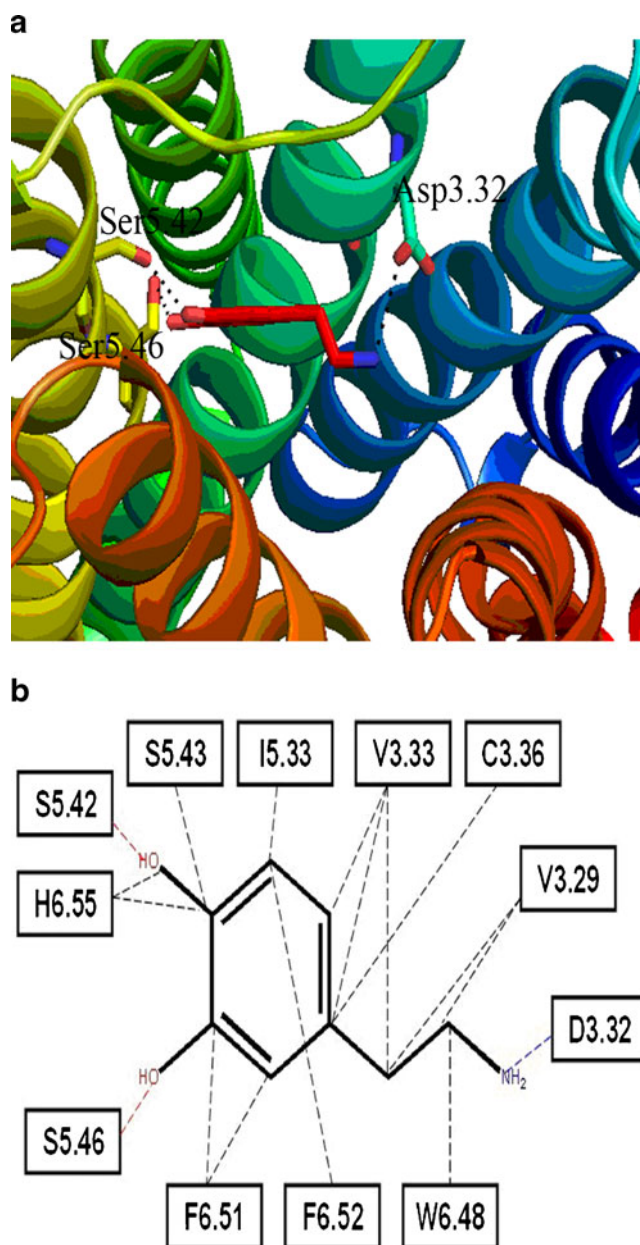


**Fig. 7** a The hydrogen bonds formed between dopamine and D3R. b Schematic view of the interactions between dopamine and D3R: hydrophobic contacts are shown in gray dashed lines, hydrogen bonds are highlighted in red, and salt bridges are highlighted in blue

during MD (Fig. 8b). Residue Tyr<sup>7.43</sup> also interacts with the ligand and the interaction remains stable. -OH(O8) of ligand interacts with Ser<sup>5.42</sup> during our MD simulation. However, we find that the hydrogen bond between Ser<sup>5.46</sup> and -OH(O7) of ligand fluctuates during our MD simulation (Fig. 8b). These results indicate that dopamine has flexibility to interact with D3R with different H-bond partners, which facilitates its role in activation of D3R.

As shown in Fig. 8a and c, hydrogen bond distances among TM127 and TM367 regions keep stable.



**Fig. 8** **a** Highly conserved residues formed inter-helical hydrogen bonds among TM127 and TM367 regions. **b** Evolution of the O-N/O-O distances between dopamine and Asp3.32, Tyr7.43, Ser5.42 and Ser5.46 for 20 ns MD simulation. **c** Evolution of the O-N/O-O distances among Asn1.50, Asp2.50, Ser3.39, Trp6.48, Asn7.45 and Ser7.46. These H-bonds are stable among TM127 and TM367 regions

Our molecular dynamics results show residues including Asp<sup>3.32</sup>, Tyr<sup>7.43</sup>, Ser<sup>5.42</sup>, Ser<sup>5.43</sup>, Ser<sup>5.46</sup> and His<sup>6.55</sup> are very important for the binding of the agonist and activation of the receptor.

Comparison between agonist-bound and antagonist-bound after MD

We make a systematic comparison between agonist-bound and antagonist-bound D3R to illustrate the structural information during the activation of D3R. Here we superimpose the structures of the agonist-bound and antagonist-bound after 20 ns MD by using PyMol.

Our results show that in three independent simulations, conformational changes are almost the same either in agonist-bound or antagonist-bound, where Fig. 9a and Fig. S11 show the similarities.

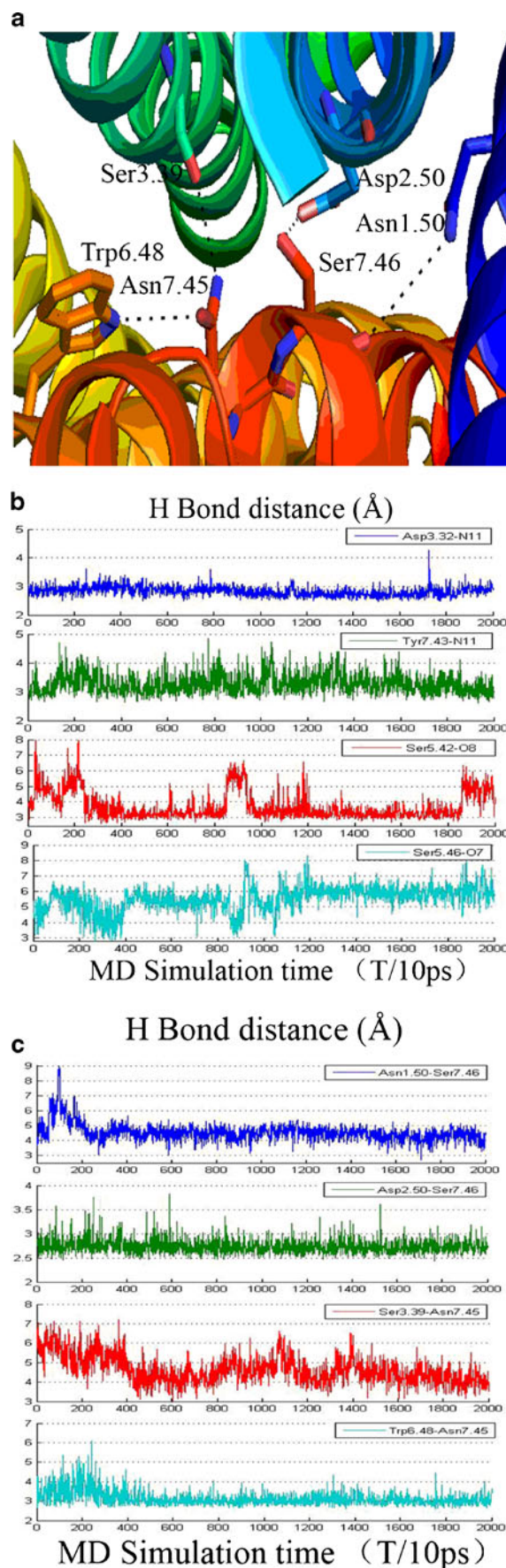
During 20 ns MD, TM1, TM2 and TM4 do not make significant deviations as described in other GPCRs [31, 38, 62–66], while TM3, TM5, TM6 and TM7 have dramatic conformational changes.

#### The unstable “ionic lock”

In the complex of D3R with antagonist, we find that TM3 slides along its axis after 20 ns MD compared with the original crystal structure of D3R. However, a larger sliding movement can be observed in the complex of D3R with agonist. Importantly, during MD of D3R with agonist, we find that “ionic lock” motif between Arg<sup>3.50</sup> of the conserved D/ERY in TM3 and highly conserved residue Glu<sup>6.30</sup> in TM6 fluctuates greatly around 18.5 ns MD in Fig. 9g (more details can be found in supplementary Fig. S12 and S5b). We think the “ionic lock” motif should be broken along with the increase of the simulation time. The residue Tyr<sup>3.60</sup>, which is considered to mediate the “ionic lock”, is also far away from them, while in the antagonist-bound, these residues interact with each other tightly, as shown in Fig. 9b and c.

#### Outward movement of TM6

Our molecular dynamic results (Fig. 9a) show that the intracellular side of TM6 moves outward, while the extracellular part moves inward. This makes “ionic lock” not favorable. TM5 moves away from TM6, and the intracellular side of



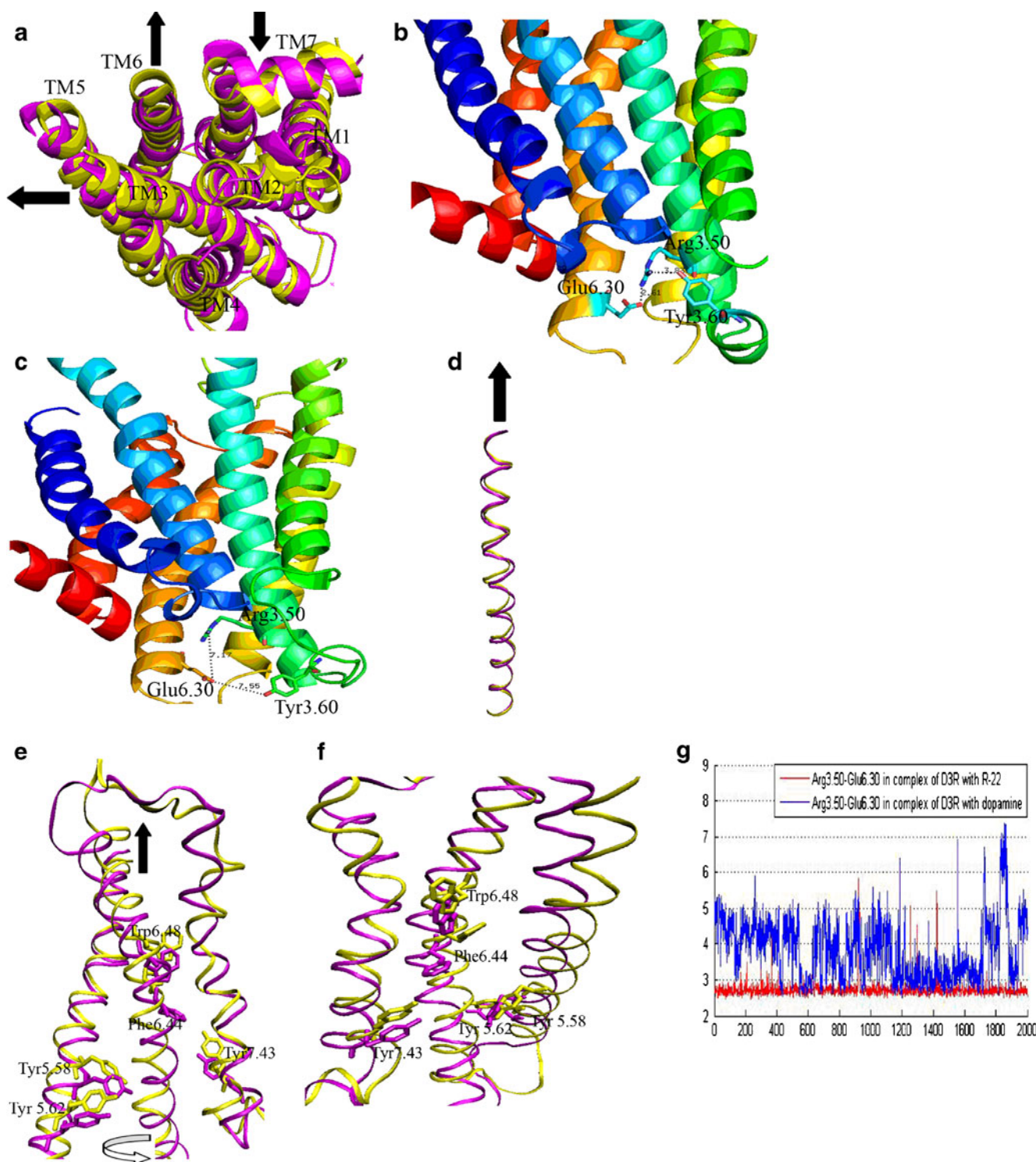


**Fig. 9** **a** Comparison of the agonist-bound with antagonist-bound. The yellow one is the agonist-bound, and the magenta one is the antagonist-bound. The arrow indicates movement of TM5, TM6, and TM7 with agonist bound. **b** The stable “ionic lock” of D3R with antagonists bound during MD. **c** The unstable “ionic lock” of D3R with dopamine bound after 18.5 ns MD. **d** Side view of the superimposed TM3. The yellow one is the agonist-bound, and the magenta one is the antagonist-bound. The arrow indicates movement of TM3 with agonist bound. **e**

Side view of the rotameric switch of conserved residues. The yellow one is the agonist-bound, and the magenta one is the antagonist-bound. The arrow indicates movement of TM6. **f** Back side view of the rotameric switch of conserved residues. The yellow one is the agonist-bound, and the magenta one is the antagonist-bound. **g** Comparison of H-bond distance evolution of Arg3.50-Glu6.30 in 20 ns MD simulation for D3R with dopamine bound or with R-22 bound



TM7 moves inward. These movements are smaller than the findings in the crystal structures as described in other GPCRs [31, 38, 62–66], but we think these movements are larger along with the increase of the simulation time.

#### *Side chain rotamer caused by the rotation and upward-movement of TM6*

As seen in Fig. 9e and f, a large change is affected by a small clockwise rotation and upward-movement of TM6. Trp<sup>6.48</sup> is highly conserved in GPCRs. It has been proposed that its rotameric state has a role in activation [31, 38, 62–66]. Our molecular dynamics illustrates no change in the side chain rotamer of Trp<sup>6.48</sup> in TM6, this agrees with the recent mutagenesis experiments on the serotonin 5HT4 receptor and the study of crystal structure of A<sub>2A</sub>AR and β<sub>2</sub> [63–66]. Our docking results and molecular dynamics results show that Trp<sup>6.48</sup> is far away from the binding pocket of ligand. Side chain rotamer of Trp<sup>6.48</sup> will be related to the distance between Trp<sup>6.48</sup> and the ligand. Side chain rotamer of Phe<sup>6.44</sup>, Tyr<sup>5.58</sup>, and Tyr<sup>5.62</sup> can be observed in TM5 and TM6. These residues have a clockwise rotation viewing from the intracellular side. These conserved residues make significant conformational change, which relates to the activation mechanism directly. We think no change in the side chain rotamer of Trp<sup>6.48</sup> in TM6 and more conformational changes can be found in residues Phe<sup>6.44</sup>, Tyr<sup>5.58</sup> and Tyr<sup>5.62</sup> along with the increase of the simulation time.

#### *Conformational change of Tyr<sup>7.53</sup>*

Conformational changes in TM7 are also important during activation mechanism. Tyr<sup>7.53</sup>, which belongs to highly conserved NPxxY motif, has a conformational change (~2.0 Å), which has been implicated in the activation mechanism of GPCRs [31, 38, 62–66]. Meanwhile, our molecular dynamics results show the backbone of NPxxY motif make significant conformational changes (~3.5 Å). We think more conformational changes can be found in residues Tyr<sup>7.53</sup> and NPxxY motif along with the increase of the simulation time.

These differences between D3R with agonist and antagonist are in agreement with the recent studies of activation mechanism [31, 38, 62–66], provide us the dynamics for the conformational transformations from inactive state to active state, and help us understand the activation mechanisms of GPCRs.

## Conclusions

Remarkable developments in pharmacology, chemistry, and neurobiology of dopamine and particularly gains of information about the molecular genetics and neuropharmacology of

dopamine receptors have been achieved over the past two decades. Despite these advances, many detailed studies of dopamine receptors and their activation mechanism remain to be worked out. The design and development of dopamine receptor-selective ligands remains largely formidable and mainly empirical, which are not ready for application of drug design. Fortunately, the crystal structure of the human D3R is reported and it provides an opportunity to understand the information of dopamine receptors.

Based on the recent available high resolution structure of human D3R, we generate homology models of three other subtypes of D<sub>2</sub>-like receptors. The structures are refined and docked to find out the important residues involved in the binding and selectivity. We perform molecular dynamics of complexes with eticlopride and R-22. Our MD simulations identify the important residues contributing to the binding and selectivity. Comparing five ligands with D3R, we find some similarities and differences among the five structures, which is critical for the ligands affinity and D3R selectivity. Finally, we dock the agonists to the receptor and compare the conformational changes between agonist-bound and antagonist-bound of D3R. We find the conformational changes which correspond to the activation mechanism of D3R. Conformational changes include (1)sliding upward of TM3, (2)outward movement of intracellular part of TM6 and inward movement of intracellular part of TM7, (3) fluctuation of “ionic lock” motif, and (4)conformational change of Tyr<sup>7.53</sup>.

**Acknowledgments** The work is supported by the National Basic Research Program of China (973 Program, Grant No. 2012CB932400 and 2010CB934500), the National Natural Science Foundation of China (Grant No. 21003091), Natural Science Foundation of Jiangsu Province (Grant No. BK2010216), a Project Funded by the Priority Academic Program Development of Jiangsu Higher Education Institutions (PAPD).

## References

- Chien EYT, Liu W, Zhao QA, Katritch V, Han GW, Hanson MA, Shi L, Newman AH, Javitch JA, Cherezov V, Stevens RC (2010) Structure of the human dopamine D3 receptor in complex with a D2/D3 selective antagonist. *Science* 330:1091–1095
- Ortore G, Tuccinardi T, Bertini S, Martinelli A (2006) A theoretical study to investigate D2DAR/D4DAR selectivity: receptor modeling and molecular docking of dopaminergic ligands. *J Med Chem* 49:1397–1407
- Heidbreder CA, Gardner EL, Xi ZX, Thanos PK, Mugnaini M, Hagan JJ, Ashby CR (2005) The role of central dopamine D-3 receptors in drug addiction: a review of pharmacological evidence. *Brain Res Rev* 49:77–105
- Ji M, Chen JY, Ding K, Wu XH, Varady J, Levant B, Wang SM (2005) Design, synthesis and structure-activity relationship studies of hexahydropyrazinoquinolines as a novel class of potent and selective dopamine receptor 3 (D-3) ligands. *Bioorg Med Chem Lett* 15:1701–1705



5. Joyce JN, Milian MJ (2005) Dopamine D-3 receptor antagonists as therapeutic agents. *Drug Discov Today* 10:917–925
6. Newman AH, Grundt P, Nader MA (2005) Dopamine D3 receptor partial agonists and antagonists as potential drug abuse therapeutic agents. *J Med Chem* 48:3663–3679
7. Sasse BC, Mach UR, Leppanen J, Calmels T, Stark H (2007) Hybrid approach for the design of highly affine and selective dopamine D-3 receptor ligands using privileged scaffolds of biogenic amine GPCR ligands. *Bioorg Med Chem* 15:7258–7273
8. Feng Z, Hou T, Li Y (2012) Studies on the interactions between  $\beta$ 2 adrenergic receptor and Gs protein by molecular dynamics simulations. *J Chem Inf Model* 52:1005–1014
9. Li Y, Hou T, Goddard I (2010) Computational modeling of structure-function of G protein-coupled receptors with applications for drug design. *Curr Med Chem* 17:1167–1180
10. Goddard WA III, Kim SK, Li Y, Trzaskowski B, Griffith AR, Abrol R (2010) Predicted 3D structures for adenosine receptors bound to ligands: comparison to the crystal structure. *J Struct Biol* 170:10–20
11. Hall DA, Strange PG (1999) Comparison of the ability of dopamine receptor agonists to inhibit forskolin-stimulated adenosine 3' 5'-cyclic monophosphate (cAMP) accumulation via D-2 L (long isoform) and D-3 receptors expressed in Chinese hamster ovary (CHO) cells. *Biochem Pharmacol* 58:285–289
12. Newman AH, Grundt P, Cyriac G, Deschamps JR, Taylor M, Kumar R, Ho D, Luedtke RR (2009) N-(4-(2,3-dichloro- or 2-methoxyphenyl)piperazin-1-yl)butyl)heterobiarylcarboxamides with functionalized linking chains as high affinity and enantioselective D3 receptor antagonists. *J Med Chem* 52:2559–2570
13. Cho DI, Zheng M, Kim KM (2010) current perspectives on the selective regulation of dopamine D-2 and D-3 receptors. *Arch Pharm Res* 33:1521–1538
14. Ortega R, Ravina E, Masaguer CF, Areias F, Brea J, Loza MI, Lopez L, Selent J, Pastor M, Sanz F (2009) Synthesis, binding affinity and SAR of new benzolactam derivatives as dopamine D-3 receptor ligands. *Bioorg Med Chem Lett* 19:1773–1778
15. Sokoloff P, Giros B, Martres MP, Bouthenet ML, Schwartz JC (1990) Molecular cloning and characterization of a novel dopamine receptor (D3) as a target for neuroleptics. *Nature* 347:146–151
16. Boeckler F, Ohnmacht U, Lehmann T, Utz W, Hubner H, Gmeiner P (2005) CoMFA and CoMSIA investigations revealing novel insights into the binding modes of dopamine D3 receptor agonists. *J Med Chem* 48:2493–2508
17. Zhang A, Neumeyer JL, Baldessarini RJ (2007) Recent progress in development of dopamine receptor subtype-selective agents: potential therapeutics for neurological and psychiatric disorders. *Chem Rev* 107:274–302
18. Boeckler F, Lanig H, Gmeiner P (2005) Modeling the similarity and divergence of dopamine D-2-like receptors and identification of validated ligand-receptor complexes. *J Med Chem* 48:694–709
19. Livingstone CD, Strange PG, Naylor LH (1992) Molecular modelling of D2-like dopamine receptors. *Biochem J* 287:277–282
20. Salama I, Hocke C, Utz W, Prante O, Boeckler F, Hubner H, Kuwert T, Gmeiner P (2007) Structure - selectivity investigations of D-2-like receptor ligands by CoMFA and CoMSIA guiding the discovery of D-3 selective PET radioligands. *J Med Chem* 50:489–500
21. Zald DH, Woodward ND, Cowan RL, Riccardi P, Ansari MS, Baldwin RM, Cowan RL, Smith CE, Hakyemez H, Li R, Kessler RM (2010) The interrelationship of dopamine D2-like receptor availability in striatal and extrastriatal brain regions in healthy humans: A principal component analysis of [ $^{18}$ F]fallypride binding. *NeuroImage* 51:53–62
22. Aujla H, Beninger RJ (2005) The dopamine D-3 receptor-preferring partial agonist BP 897 dose-dependently attenuates the expression of amphetamine-conditioned place preference in rats. *Behav Pharmacol* 16:181–186
23. Beardsley PM, Sokoloff P, Balster RL, Schwartz JC (2001) The D3R partial agonist, BP 897, attenuates the discriminative stimulus effects of cocaine and D-amphetamine and is not self-administered. *Behav Pharmacol* 12:1–11
24. Garcia-Ladona FJ, Cox BF (2003) BP 897, a selective dopamine D-3 receptor ligand with therapeutic potential for the treatment of cocaine-addiction. *CNS Drug Rev* 9:141–158
25. Wicke K, Garcia-Ladona J (2001) The dopamine D3 receptor partial agonist, BP 897, is an antagonist at human dopamine D3 receptors and at rat somatodendritic dopamine D3 receptors. *Eur J Pharmacol* 424:85–90
26. Wood MD, Boyfield I, Nash DJ, Jewitt FR, Avenell KY, Riley GJ (2000) Evidence for antagonist activity of the dopamine D3 receptor partial agonist, BP 897, at human dopamine D3 receptor. *Eur J Pharmacol* 407:47–51
27. Clement P, Pozzato C, Heidbreder C, Denys P, Giuliano F, Melotto S (2009) Sb-277011, a selective dopamine D3 receptor antagonist, delays ejaculation in conscious and anesthetized rats. *Eur Urol Suppl* 8:365–365
28. Dravolina OA, Shekunova EV, Zvartau EE, van Gaalen MM, Drescher KU, Schoemaker H, Gross G, Beshpalov AY (2007) Effects of the selective dopamine D3 receptor antagonist SB-277011 on cue- and nicotine-induced relapse to nicotine-seeking behavior. *Behav Pharmacol* 18:S87–S87
29. Gilbert JG, Newman AH, Gardner EL, Ashby CR, Heidbreder CA, Pak AC, Peng XQ, Xi ZX (2005) Acute administration of SB-277011A, NGB 2904, or BP 897 inhibits cocaine cue-induced reinstatement of drug-seeking behavior in rats: Role of dopamine D-3 receptors. *Synapse* 57:17–28
30. Khaled MATM, Araki KF, Li B, Coen KM, Marinelli PW, Varga J, Gaal J, Le Foll B (2010) The selective dopamine D-3 receptor antagonist SB 277011-A, but not the partial agonist BP 897, blocks cue-induced reinstatement of nicotine-seeking. *Int J Neuropsychoph* 13:181–190
31. Reavill C, Taylor SG, Wood MD, Ashmeade T, Austin NE, Avenell KY, Boyfield I, Branch CL, Cilia J, Coldwell MC, Hadley MS, Hunter AJ, Jeffrey P, Jewitt F, Johnson CN, Jones DNC, Medhurst AD, Middlemiss DN, Nash DJ, Riley GJ, Routledge C, Stemp G, Thewlis KM, Trail B, Vong AKK, Hagan JJ (2000) Pharmacological actions of a novel, high-affinity, and selective human dopamine D-3 receptor antagonist, SB-277011-A. *J Pharmacol Exp Ther* 294:1154–1165
32. Spiller K, Xi ZX, Peng XQ, Newman AH, Ashby CR, Heidbreder C, Gaal J, Gardner EL (2008) The selective dopamine D-3 receptor antagonists SB-277011A and NGB 2904 and the putative partial D-3 receptor agonist BP-897 attenuate methamphetamine-enhanced brain stimulation reward in rats. *Psychopharmacology* 196:533–542
33. Thanos PK, Katana JM, Ashby CR, Michaelides M, Gardner EL, Heidbreder CA, Volkow ND (2005) The selective dopamine D3 receptor antagonist SB-277011-A attenuates ethanol consumption in ethanol preferring (P) and non-preferring (NP) rats. *Pharmacol Biochem Be* 81:190–197
34. Thanos PK, Michaelides M, Ho CW, Wang GJ, Newman AH, Heidbreder CA, Ashby CR, Gardner EL, Volkow ND (2008) The effects of two highly selective dopamine D-3 receptor antagonists (SB-277011A and NGB-2904) on food self-administration in a rodent model of obesity. *Pharmacol Biochem Be* 89:499–507
35. Martelle JL, Claytor R, Ross JT, Reboussin BA, Newman AH, Nader MA (2007) Effects of two novel D-3-selective compounds, NGB 2904 [N-(4-(2,3-dichlorophenyl)piperazin-1-yl)butyl]-9 H-fluorene-2-carboxamide] and CJB 090 [N-(4-(2,3-dichlorophenyl)piperazin-1-yl)butyl]-4-(pyridin-2-yl)benzamide], on the reinforcing and discriminative stimulus effects of cocaine in rhesus monkeys. *J Pharmacol Exp Ther* 321:573–582

36. Xi ZX, Gardner EL (2007) Pharmacological actions of NGB 2904, a selective dopamine D-3 receptor antagonist, in animal models of drug addiction. *CNS Drug Rev* 13:240–259
37. Xi ZX, Newman AH, Gilbert JG, Pak AC, Peng XQ, Ashby CR, Gitajn L, Gardner EL (2006) The novel dopamine D-3 receptor antagonist NGB 2904 inhibits cocaine's rewarding effects and cocaine-induced reinstatement of drug-seeking behavior in rats. *Neuropsychopharmacology* 31:1393–1405
38. Stefan L, Harald H, Nuska T, Gmeiner P (2011) Recent advances in the search for D<sub>3</sub>- and D<sub>4</sub>-selective drugs: probes, models and candidates. *Trends Pharmacol Sci* 32:148–157
39. Silvano E, Millan MJ, la Cour CM, Han Y, Duan LH, Griffin SA, Luedtke RR, Aloisi G, Rossi M, Zazzeroni F, Javitch JA, Maggio R (2010) The tetrahydroisoquinoline derivative SB269,652 is an allosteric antagonist at dopamine D-3 and D-2 receptors. *Mol Pharmacol* 78:925–934
40. Taylor S, Riley G, Hunter A, Stemp G, Routledge C, Hagna JCR (1999) SB269,652 is a selective D3 receptor antagonist in vitro and in vivo. *J Eur College Neuropsychopharmacol* 9:S266
41. Studio D (2007) version 2.5. Accelrys Inc.: San Diego, CA
42. Wiederstein M, Sippl MJ (2007) ProSA-web: interactive web service for the recognition of errors in three-dimensional structures of proteins. *Nucleic Acids Res* 35:W407–W410
43. Laskowski RA, Rullmann JAC, MacArthur MW, Kaptein R, Thornton JM (1996) AQUA and PROCHECK-NMR: programs for checking the quality of protein structures solved by NMR. *J Biomol NMR* 8:477–486
44. Pettersen EF, Goddard TD, Huang CC, Couch GS, Greenblatt DM, Meng EC, Ferrin TE (2004) UCSF Chimera—a visualization system for exploratory research and analysis. *J Comput Chem* 25:1605–1612
45. Brooks BR, Brucoleri RE, Olafson BD (1983) CHARMM: A program for macromolecular energy, minimization, and dynamics calculations. *J Comput Chem* 4:187–217
46. Jorgensen WL, Chandrasekhar J, Madura JD, Impey RW, Klein ML (1983) Comparison of simple potential functions for simulating liquid water. *J Chem Phys* 79:926
47. Humphrey W, Dalke A, Schulten K (1996) VMD: visual molecular dynamics. *J Mol Graph* 14:33–38
48. Li Y, Hou T (2010) Computational simulation of drug delivery at molecular level. *Curr Med Chem* 17:4482–4491
49. Kim SK, Li Y, Abrol R, Heo J, Goddard WA III (2011) Predicted structures and dynamics for agonists and antagonists bound to serotonin 5-HT<sub>2B</sub> and 5-HT<sub>2C</sub> receptors. *J Chem Inf Model* 51:420–433
50. Li Y, Zhu F, Vaidehi N, Goddard WA III, Sheinerman F, Reiling S, Morize I, Mu L, Harris K, Ardati A (2007) Prediction of the 3D structure and dynamics of human DP G-protein coupled receptor bound to an agonist and an antagonist. *J Am Chem Soc* 129:10720–10731
51. Kim SK, Li Y, Park C, Abrol R, Goddard WA III (2010) Prediction of the three-dimensional structure for the rat urotensin ii receptor, and comparison of the antagonist binding sites and binding selectivity between human and rat receptors from atomistic simulations. *Chem Med Chem* 5:1594–1608
52. Kalé L, Skeel R, Bhandarkar M, Brunner R, Gursoy A, Krawetz N, Phillips J, Shinozaki A, Varadarajan K, Schulten K (1999) NAMD2: greater scalability for parallel molecular dynamics\* 1. *J Comput Phys* 151:283–312
53. MacKerell AD, Bashford D, Bellott M, Dunbrack RL, Evanseck JD, Field MJ, Fischer S, Gao J, Guo H, Ha S, Joseph-McCarthy D, Kuchnir L, Kuczera K, Lau FTK, Mattos C, Michnick S, Ngo T, Nguyen DT, Prodhom B, Reiher WE, Roux B, Schlenkrich M, Smith JC, Stote R, Straub J, Watanabe M, Wiorkiewicz-Kuczera J, Yin D, Karplus M (1998) All-atom empirical potential for molecular modeling and dynamics studies of proteins. *J Phys Chem B* 102:3586–3616
54. Feller SE, MacKerell AD (2000) An improved empirical potential energy function for molecular simulations of phospholipids. *J Phys Chem B* 104:7510–7515
55. Essmann U, Perera L, Berkowitz ML, Darden T, Lee H, Pedersen LG (1995) A smooth particle mesh Ewald method. *J Chem Phys* 103:8577–8593
56. Plesnar E, Subczynski WK, Pasenkiewicz-Gierula M (2012) Saturation with cholesterol increases vertical order and smoothes the surface of the phosphatidylcholine bilayer: a molecular simulation study. *BBA-Biomembranes* 1818:520–529
57. Kalani MYS, Vaidehi N, Hall SE, Trabanino RJ, Freddolino PL, Kalani MA, Floriano WB, Kam VWT, Goddard WA (2004) The predicted 3D structure of the human D2 dopamine receptor and the binding site and binding affinities for agonists and antagonists. *Prog Natl Acad Sci USA* 101:3815–3820
58. Zhang P, Cyriac G, Kopajtic T, Zhao YF, Javitch JA, Katz JL, Newman AH (2010) structure-ACTIVITY relationships for a novel series of citalopram (1-(3-(Dimethylamino)propyl)-1-(4-fluorophenyl)-1,3-dihydroisobenzofuran-5-carbonitrile) analogues at monoamine transporters. *J Med Chem* 53:6112–6121
59. Soriano-Ursúa MA, Ocampo-López JO, Ocampo-Mendoza K, Trujillo-Ferrara JG, Correa-Basurto J (2011) Theoretical study of 3-D molecular similarity and ligand binding modes of orthologous human and rat D2 dopamine receptors. *Comput Biol Med* 41:537–545
60. Andujar S, Tosso R, Suvire FD, Angelina EL, Peruchena N, Cabedo N, Cortes D, Enriz RD (2012) Searching the “biologically relevant” conformation of dopamine, a computational approach. *J Chem Inf Model* 52:99–112
61. Zhao YX, Lu XF, Yang CY, Huang ZM, Fu W, Hou TJ, Zhang JA (2010) Computational modeling toward understanding agonist binding on dopamine 3. *J Chem Inf Model* 50:1633–1643
62. Lebon G, Warne T, Edwards PC, Bennett K, Langmead CJ, Leslie AG, Tate CG (2011) Agonist-bound adenosine A2A receptor structures reveal common features of GPCR activation. *Nature* 474:521–525
63. Rasmussen SG, Choi HJ, Fung JJ, Pardon E, Casarosa P, Chae PS, Devree BT, Rosenbaum DM, Thian FS, Kobilka TS, Schnapp A, Konetzki I, Sunahara RK, Gellman SH, Pautsch A, Steyaert J, Weis WI, Kobilka BK (2011) Structure of a nanobody-stabilized active state of the beta(2) adrenoceptor. *Nature* 469:175–180
64. Standfuss J, Edwards PC, Antona AD, Franssen M, Xie G, Oprian DD, Schertler GFX (2011) The structural basis of agonist-induced activation in constitutively active rhodopsin. *Nature* 471:656–660
65. Vignir I, Thomas B, Tommy S, Jørgensen FS, Isberg DEV (2011) G Protein- and agonist-bound serotonin 5-HT<sub>2A</sub> receptor model activated by steered molecular dynamics simulations. *J Chem Inf Model* 51:315–325
66. Xu F, Wu H, Katritch V, Han G, Jacobson K, Gao Z, Cherezov V, Stevens R (2011) Structure of an agonist-bound human a2a adenosine receptor. *Science* 332:322–327